

Swirling Flow Effect on Film Cooling Performance Downstream of a Sudden Expansion

C. Gau,* K. A. Yih,† and S. S. Chang†

National Cheng Kung University, Tainan, Taiwan, Republic of China

Experiments are performed to study and obtain the film cooling effectiveness in a film cooled circular pipe downstream of an abrupt 2.4:1 expansion with the presence of weak swirling flow in the mainstream. The swirling flow is generated by a flat-vaned swirler situated upstream before expansion. The radial temperature measurements are used to infer the flow structure and the rate of mixing of film jet with swirling flow. Experiments demonstrate that the size of the recirculation zone and the location of the reattachment point are significantly affected by the swirl and the film jet velocity. The recirculation zone has a very slow rate of mixing with film jet and results in a higher film cooling effectiveness. However, the reattachment of flow can impinge and destroy severely the film jet structure and results in a significant reduction in film cooling effectiveness. The system of governing equations and boundary conditions are used to derive the dimensionless parameters that affect the film cooling performance. In the experiments, the blowing parameter ranged from 0.5 to 2.0, and the swirl number from 0 to 0.6. Correlations for film cooling effectiveness are presented.

Nomenclature

D_h	= diameter of swirl hub
D_s	= inside diameter of swirler
f	= function
k	= conductivity
M	= blowing parameter, $= u_j/u_m$
P	= dimensionless pressure, $= p/\rho u_m^2$
Pr	= Prandtl number
p	= pressure
Q	= dimensionless heat flux, $= q/[k(T_j - T_m)/R_o]$
q	= heat flux
R	= dimensionless distance, $= r/y_c$
R_o	= pipe radius after expansion
Re_s	= slot Reynolds number, $= \rho u_m y_c / \mu$
r	= radial coordinate
r_h	= swirl hub radius
r_o	= pipe radius before expansion
r_s	= swirler radius, $= r_o$
S	= swirl number
T	= temperature
U	= dimensionless velocity in the x direction, $= u/u_m$
u	= fluid velocity in the x direction
u_m	= average velocity of the mainstream in the x direction
V	= dimensionless velocity in the r direction, $= v/u_m$
v	= fluid velocity in the r direction
w	= fluid velocity in the ψ direction
X	= dimensionless distance, $= x/y_c$
x	= axial distance from slot
y	= radial distance from pipe wall
y_c	= slot height
η	= film cooling effectiveness, $= (T_{aw} - T_m)/(T_j - T_m)$
Θ	= dimensionless temperature, $= (T - T_m)/(T_j - T_m)$
μ	= kinematic viscosity
Φ	= vane angle of swirler
ψ	= circumferential coordinate

Subscripts

aw	= adiabatic wall
j	= film jet at slot exit
m	= mainstream

Introduction

FILM cooling heat transfer has been studied extensively in the past due to its wide applications in cooling high-temperature systems such as combustors, turbines blades, afterburners, and nozzles. Extensive review articles on both analytical and experimental studies on film cooling heat transfer are available.^{1,2} The film cooling effectiveness has been well-correlated with the blowing parameter and the downstream distance. However, the results obtained in the past are used only for the case in which the hot flow over a film cooled flat surface is uniform and both the mainstream and the film jet have a very low-turbulence intensity. Recent studies have indicated that different flow configurations, such as a favorable or an adverse pressure gradient in the mainstream,^{3,4} the turbulence intensity in either the mainstream or the film jet,^{5,6} the surface roughness,⁷ and the surface curvature⁸ of the wall, which may be frequently encountered in a practical application, can have a significant effect on the film cooling performance and the heat-transfer process under the film. These effects should be carefully examined. For a swirling flow through a film cooled pipe without expansion, Gau and Hwang⁹ found that the swirl number, which increases with turbulence intensity and swirl velocity in the mainstream,^{10,11} can significantly increase the mixing rate of the film jet with swirl flow and decrease the film cooling effectiveness. The film cooling effectiveness has been correlated in terms of the swirl number, the blowing parameter, and the downstream distance.

In a dump combustor of gas turbine engine or a solid fuel ramjet combustor, air is usually swirled to enhance its rate of mixing with fuel droplets and increase the combustion efficiency and, at the same time, is expanded suddenly to create a recirculation region for flame holding. The structure of swirling flow has been studied extensively due to its complex phenomenon and its effect on the combustion efficiency.¹⁰⁻¹² However, only a relatively few works^{13,14} deal with the effect of suddenly expanded swirling flow on the heat transfer rate along the wall. The heat transfer rate on the wall was found to increase with the swirl. In the meantime, as swirl increases, a sharply peaked behavior of maximum heat transfer appears, and the location of peak heat transfer rate shifts upstream due to the upstream movement of the reattachment point. Therefore, it is expected that the suddenly expanded swirling flow can have a significant effect on the film cooling performance on the wall. However, an extensive review of the literature

Received Aug. 28, 1989; revision received Jan. 23, 1990; accepted for publication Feb. 15, 1990. Copyright © 1989 by the American Institute of Aeronautics and Astronautics, Inc. All rights reserved.

*Associate Professor, Institute of Aeronautics and Astronautics.

†Graduate Student, Institute of Aeronautics and Astronautics.

indicates that these effects have been overlooked in the past and should be examined carefully. Therefore, the objective of this work is to study and obtain film cooling data downstream of an abrupt expansion of a swirling flow. The radial temperature distributions at several locations are measured and used to infer the flow structure and the rate of mixing of the film jet with the mainstream. Before the experiments, a nondimensional analysis is used to derive the dimensionless parameters that affect the film cooling effectiveness. Correlations for film cooling effectiveness that account for the effect of a suddenly expanded swirl flow are presented.

Experimental Apparatus

Experiments are performed in an open-type wind tunnel. The test section, as shown in Fig. 1, is a circular Plexiglas pipe and is 90 cm in length, 30 cm in inside diameter, and 1 cm in wall thickness. The velocity of uniform airflow is maintained at desirable values, and the maximum turbulence intensity is kept within 0.4%. The turbulence intensity was measured with a hot-wire anemometer at the outlet of the contraction and upstream of the swirler. A single, flat-vaned swirler, having both vane aspect ratio and space-chord ratio of approximately unity, is located at the outlet of the circular contraction to generate swirling flow. After passing through the swirler, the airflow is suddenly expanded into a large pipe, having an expansion of diameter ratio of 2.4. The secondary heated air is injected axially from an annular slot formed by the pipe wall and a cover plate. The slot height at exit is 4 mm.

All of the swirlers used are actually the same as those described in the previous work.⁹ The swirler is made of stainless steel and has 10 pieces of 1-mm-thick flat vanes. A total of seven different swirlers, having inside diameter of 12.4 cm and hub diameter of 5 cm, were made. The vane angles of these swirlers are 0, 7.7, 15, 22, 28, 34, and 39 deg, respectively. However, the generated swirling flow is usually characterized by the swirl number S , which is a nondimensional parameter representing the axial flux of swirl momentum divided by the product of axial flux of axial momentum and swirl radius. It has been obtained¹⁰ that the swirl vane angle and the swirl number are related by

$$S = \frac{2}{3} \tan \Phi [1 - (D_h/D_s)^3] / [1 - (D_h/D_s)^2] \quad (1)$$

Accordingly, the swirl number of the swirling flow made by each of these swirlers is 0, 0.1, 0.2, 0.3, 0.4, 0.5, and 0.6, respectively. To avoid flow recirculation and generation of turbulence before the air enters the swirler, a guide cone is placed in front of the hub, as shown in Fig. 1.

The secondary air is filtered and pumped by a centrifugal blower with its blade rotation speed controlled by a frequency transistor. After passing through the heater and a flow straightener, the heated air is distributed into 25 small insulated tubes, that are made equal in length and are connected to a plenum chamber of annular shape. The plenum chamber is used to reduce the turbulence intensity and enables the air to leave the slot uniformly so that a film jet of uniform injection velocity can be obtained. The temperature of the film jet at the exit of the slot is maintained 20°C higher than that of the mainstream. To reduce the heat loss, the entire test section is well insulated with a 25-mm-thick porous material of low conductivity ($k = 0.049$ W/m-K).

A total of 45 thermocouples are embedded into the pipe wall to measure the adiabatic temperature distribution of the wall in the axial direction. The junctions of the thermocouples are kept at the wall surface. The pitch between adjacent thermocouples is 4 mm except that the first thermocouple is located 8 mm from the slot exit. A total of another 24 thermocouples, having a wire diameter of 0.05 in., are made into a rake, which can be inserted into the pipe wall, to measure the radial temperature distributions. The rake has an outside diameter of 4 mm, which is relatively small as compared with the pipe with expansion. It is expected that the insertion of the small rake

does not have a significant effect on the flowfield. A closer spacing is made of thermocouples near the wall where the temperature may have larger variations. The pitch between adjacent thermocouples near the wall is 2 mm. Further away from the wall, the pitches are 4, 6, and 8 mm, respectively, increasing in the direction toward the pipe center. The temperatures of the injected and the mainstream air are also measured. All the thermocouples used in the experiment are K-type, which have been calibrated with a constant temperature bath and have a measurement accuracy of $\pm 0.1^\circ\text{C}$.

Nondimensional Analysis

To find the proper nondimensional parameters in such a complicated system that affect the film cooling performance, one has to start from the governing equations and boundary conditions of the system and perform a nondimensional analysis. The analysis can be simplified greatly by the assumption that the flow is laminar and all the thermophysical properties are constant. Further simplification can be made by the application of the boundary-layer approximation.¹⁰ With the following nondimensional parameters

$$X = x/y_c, \quad R = r/y_c, \quad u/u_m$$

$$V = v/u_m, \quad W = w/w_m, \quad P = p/\rho u_m^2$$

$$\Theta = (T - T_m)/(T_j - T_m), \quad Q = q/[k(T_j - T_m)/R_o]$$

the nondimensional boundary-layer equations and boundary conditions can be written as

Continuity:

$$\frac{\partial U}{\partial X} + \frac{1}{R} \frac{\partial(RV)}{\partial R} + \frac{1}{R} \frac{\partial W}{\partial \psi} = 0 \quad (2)$$

Momentum:

$$U \frac{\partial U}{\partial X} + V \frac{\partial U}{\partial R} + \frac{W}{R} \frac{\partial W}{\partial \psi} = -\frac{\partial P}{\partial X} + \frac{1}{Re_s} \times \left[\frac{1}{R} \frac{\partial}{\partial R} \left(R \frac{\partial U}{\partial R} \right) + \frac{1}{R^2} \frac{\partial^2 U}{\partial \psi^2} \right] \quad (3)$$

$$\frac{W^2}{R} = \frac{\partial P}{\partial R} \quad (4)$$

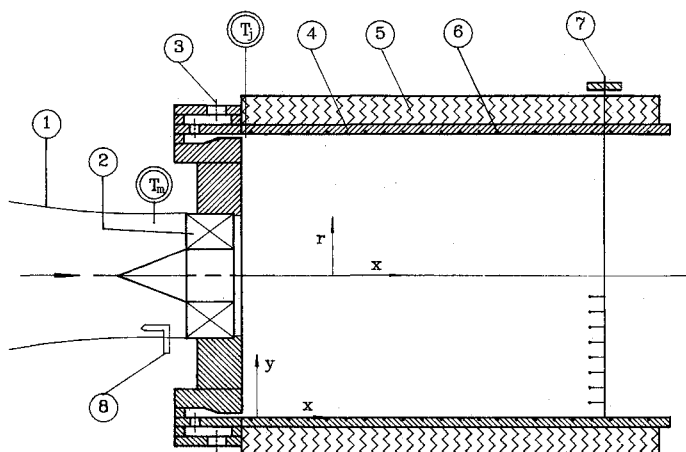


Fig. 1 Schematic diagram of test section: 1) contraction, 2) flat-vaned swirler, 3) film flow inlet, 4) adiabatic wall, 5) insulation, 6) thermocouple, 7) thermocouple rack, 8) pitot tube.

$$U \frac{\partial W}{\partial X} + V \frac{\partial W}{\partial R} + \frac{W}{R} \frac{\partial W}{\partial \psi} + \frac{VW}{R} = -\frac{1}{R} \frac{\partial P}{\partial \psi} + \frac{1}{Re_s} \frac{1}{R^2} \frac{\partial}{\partial R} \left[R^3 \frac{\partial}{\partial R} \left(\frac{W}{R} \right) \right] \quad (5)$$

Energy:

$$U \frac{\partial \Theta}{\partial X} + V \frac{\partial \Theta}{\partial R} + \frac{W}{R} \frac{\partial \Theta}{\partial \psi} = \frac{1}{Re_s Pr} \frac{1}{R} \frac{\partial}{\partial R} \left(R \frac{\partial \Theta}{\partial R} \right) \quad (6)$$

Boundary conditions:

$$X = 0, 0 < R < r_h/y_c: U = V = W = 0, \Theta = 0 \quad (7a)$$

$$X = 0, r_h/y_c < R < r_s/y_c: U = 1, V = 0, W = w_\psi/u_m, \Theta = 0 \quad (7b)$$

$$X = 0, r_s/y_c < R < (R_o - y_c)/y_c: U = V = W = 0, \Theta = 0 \quad (7c)$$

$$X = 0, (R_o - y_c) < R < R_o/y_c: U = M, V = W = 0, \Theta = 1 \quad (7d)$$

$$R = R_o/y_c: U = V = W = 0, \Theta = 0, Q = 0 \quad (7e)$$

Since $\eta_{aw} = (T_{aw} - T_m)/(T_j - T_m) = \Theta|_{R=R_o/y_c, Q=0}$, one has

$$\eta_{aw} = f(Re_s, X, M, Pr, w_\psi/u_m, r_h/y_c, r_s/y_c, R_o/y_c) \quad (8)$$

To reduce the number of parameters that affect the film cooling effectiveness, the last three parameters are divided by r_s/y_c . Therefore, $\eta_{aw} = f(Re_s, X, M, Pr, w_\psi/u_m, r_h/r_s, R_o/r_s)$.

The swirl number increases with the turbulence intensity and swirl velocity produced in the mainstream. In the experiments, it is convenient to use the swirl number to account for these effects. Besides, from Eq. (1), the swirl number can also account for the effect of the radius ratio r_h/r_s . Therefore, both the parameters w_ψ/u_m and r_h/r_s in the previous equations are replaced by the swirl number that is used as one of the dimensionless parameters for presentation and correlation of results. This leads to $\eta_{aw} = f(Re_s, X, M, Pr, S, R_o/r_s)$. Since both Pr and the expansion ratio R_o/r_s remain constant in the experiments, one can write

$$\eta_{aw} = f(Re_s, X, M, S) \quad (9)$$

Results and Discussion

Temperature Distribution Measurements

The radial temperature measurements at several axial locations are used to infer the flow structure and the rate of mixing

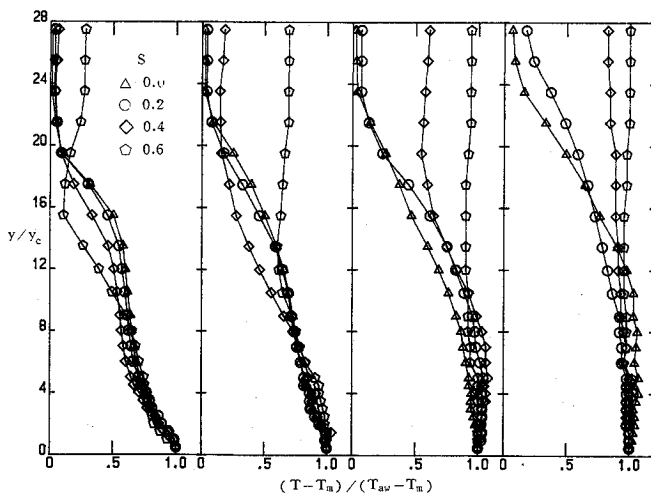


Fig. 2 Effect of swirl on the dimensionless temperature distribution for $M=1.0$: a) $x/y_c = 6$; b) $x/y_c = 24$; c) $x/y_c = 36$; and d) $x/y_c = 60$.

of the film jet with the swirling flow at different swirl numbers, as shown in Figs. 2 and 3, and at different blowing parameters, as shown in Figs. 4. The slot Reynolds number studied is at 3.93×10^3 . Close to the slot region ($x/y_c = 6$), the film jet structure is preserved, as shown in Figs. 2a–4a; however, it does not resemble that for the case of the swirling flow in a film cooled pipe without expansion, which has a higher dimensionless temperature gradient near the wall.¹⁵ This is attributed to the recirculation zone, which has a higher temperature due to the mixing with the film jet. As the recirculation zone has a direct contact with the film jet, the structure of the recirculation flow has a significant effect on the rate of mixing of the film jet with the mainstream. It is desirable to describe the structure of recirculation flow.

It has been realized that for the flow passing through the backward facing step, the flow expands, recirculates, and reattaches to the wall. A recirculation zone usually forms in the corner of the sudden expansion.^{16,17} The recirculation zone usually has relatively low velocity and turbulence intensity. However, the flow structure, turbulence intensity, and size of the recirculation zone can be significantly affected by both the swirl in the mainstream and the film jet velocity along the wall. The recirculation zone and the film jet structure can be identified from the dimensionless temperature distribution upstream, where the film jet still maintains its structure and does not mix well with the outside flow. The size of the recirculation zone for the case of $S \leq 0.2$ can be inferred, as shown in

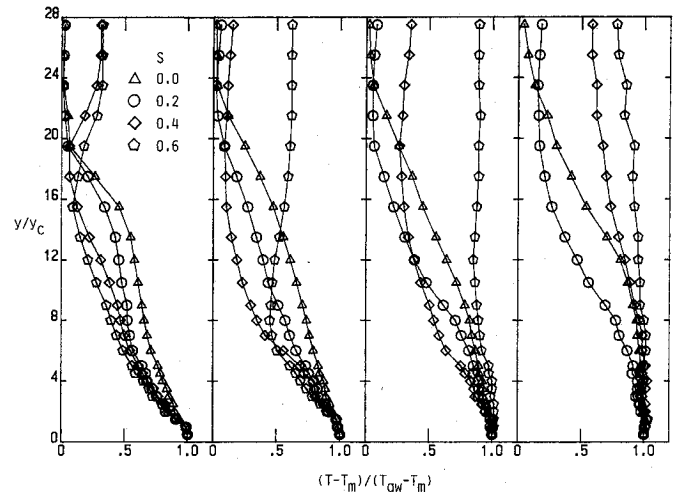


Fig. 3 Effect of swirl on the dimensionless temperature distribution for $M=2.0$: a) $x/y_c = 6$; b) $x/y_c = 24$; c) $x/y_c = 36$; and d) $x/y_c = 60$.

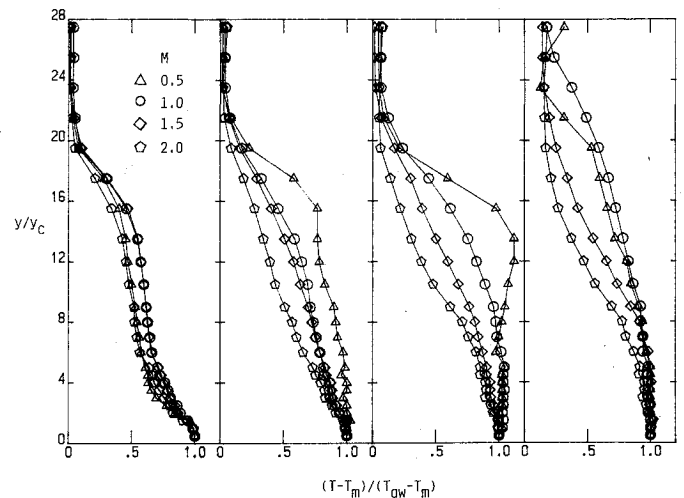


Fig. 4 Effect of blowing parameter on the dimensionless temperature distribution for $S=0.2$: a) $x/y_c = 6$; b) $x/y_c = 24$; c) $x/y_c = 36$; and d) $x/y_c = 60$.

Fig. 2a for the case of $M = 1$, in the region approximately from $y/y_c = 4$ to 16, where the variation of temperature is small. The shear layer, which can be identified in the region where the dimensionless temperature gradient is slightly higher, forms in the region from $y/y_c = 16$ to 20 (the step height is at $y/y_c = 20$) outside of the recirculation zone, and the region from $y/y_c = 1$ to 4 between the film jet and the recirculation zone. However, the inflection point of the dimensionless temperature profile, which is identified as the edge of the shear layer, moves toward the wall when the flow moves downstream. At $x/y_c = 60$, the inflection point moves upward, which indicates the redevelopment of flow after the reattachment. Therefore, the size of the recirculation zone can be inferred and the length of the recirculation is less than $x/y_c = 60$. It is worth noting, from Figs. 2a and 3a, that the height of the shear layer outside of the recirculation decreases with an increase in the swirl number. This suggests that the recirculation zone shrinks as the swirl of flow increases. For example, in Fig. 2a, the edge of the recirculation zone is approximately at $y/y_c = 15$ for both $S = 0, 0.2$, at $y/y_c = 13$ for $S = 0.4$, and at $y/y_c = 8$ for $S = 0.6$. The shrinking of the recirculation zone with increasing swirl number was also concluded by others.^{10,18} On the other hand, the effect of the blowing parameter on the recirculation flow is not significant for $S = 0$ until downstream where the film jet structure may have been significantly destroyed¹⁵ and becomes significant when the mainstream is swirled, as shown in Fig. 4. The size of the recirculation zone decreases as the blowing parameter increases, which can be clearly inferred from Fig. 4. It appears that an increase in the film jet velocity can change the entire flow structure and causes the reduction of the recirculation zone only when the mainstream is swirled.

The reattachment of flow plays a very important role to affect the film cooling performance. It is expected that the reattachment of flow, which may accompany high-swirl velocity and high-turbulence intensity, can severely destroy the film jet structure and enhance the rate of mixing of the film jet with the mainstream. However, the shrinking of the recirculation zone can move the reattachment point upstream. Therefore, the increase in either the swirl number or the blowing parameter can reduce the length of reattachment and, hence, can cause an earlier destruction of the film jet structure.

The rapid mixing of the film jet with the swirling flow also can be inferred from the rate of diffusion of temperature from the wall, as shown in Figs. 2-4. The rate of diffusion of temperature from the wall increases with the swirl number. A uniform temperature distribution in the region near the wall can be observed, e.g., for $M = 1.0$ at $x/y_c = 36$ in Fig. 2, which suggests that the film jet structure has been completely destroyed at this stage. However, the increase in the blowing parameter can make the complete destruction of the film jet occur at a later stage. The complete destruction of the film jet structure has also been found for the case of the swirling flow in a film cooled pipe without expansion⁹ and was attributed to the swirl velocity and turbulence intensity in the swirling flow, which can rapidly destroy the film jet structure.

For a high degree of swirling flow ($S = 0.6$), the dimensionless temperature near the entrance in the central region from $y/y_c = 20$ to the pipe center ($y/y_c = 37.5$) is slightly higher, as shown in Figs. 2a and 3a. This phenomenon can be attributed to the presence of the so-called central toroidal recirculation zone (CTRZ).^{16,19,20} The thermal energy in the downstream is carried backward by the recirculated flow in a CTRZ, which causes a higher temperature in the entrance. A CTRZ is formed when the so-called vortex breakdown occurs^{16,19} and the axial momentum of the swirling flow is unable to overcome the adverse axial pressure gradient (when the swirl increases, the axial momentum decreases and the adverse axial pressure gradient increases). When the blowing parameters increase, as shown in Fig. 3a, a CTRZ is formed at a lower swirl number, i.e., $S = 0.4$. It appears that the high axial momentum of the film jet plays an important role in increas-

ing the adverse axial pressure gradient downstream and causes the vortex breakdown to occur.

Film Cooling Effectiveness

The film cooling effectiveness measured at various blowing parameters in the absence of the swirling flow is compared with the empirical equations of Ko and Liu²¹ for the case of the film cooling over a flat plate, and the data of Gau and Hwang⁹ for a film cooled pipe without expansion, as shown in Figs. 5a and 5b. Significant difference in film cooling effectiveness can be observed. The effectiveness for the present data is significantly higher in the near slot region and lower in the downstream region than that of Ko and Liu.²¹ This higher film cooling effectiveness in the near slot region can be attributed to the occurrence of relatively weak recirculation flow, that the effective blowing ratio of the film jet velocity to the recirculation velocity is relatively high and the mixing process between the film jet and the mainstream is weak. The lower film cooling effectiveness in the downstream region is attributed to the reattachment of flow, which can impinge and severely destroy the film jet structure. When the blowing parameter is high, the film jet has a higher velocity and its structure is strong; therefore, the reattachment of flow cannot effectively destroy its structure. In addition, due to the high axial momentum of the film jet, the reattachment point is expected to move downstream. This downstream movement of the reattachment point slows down the impinging velocity of flow and results in a higher film cooling effectiveness. Figure 5b shows that the film cooling effectiveness increases monotonically with the blowing parameter and reaches a con-

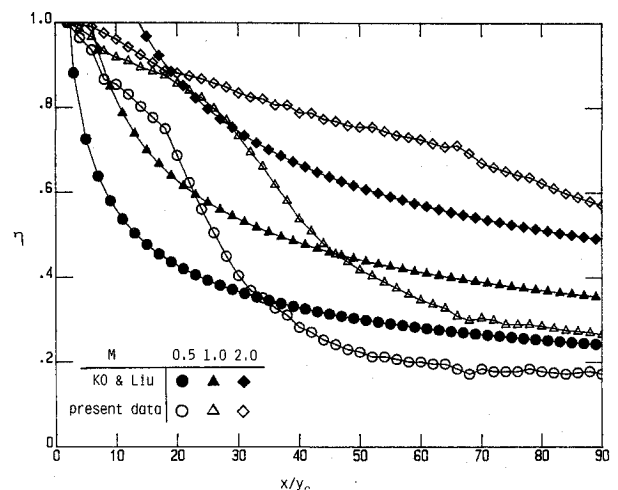


Fig. 5a Comparison of film cooling effectiveness with that of previous results for η vs x/y_c .

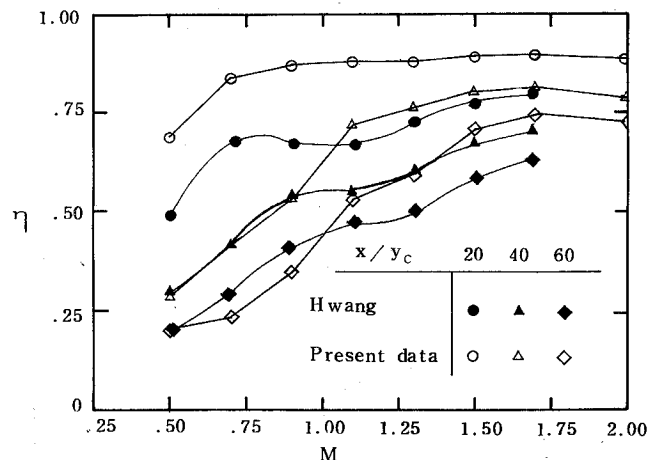


Fig. 5b Comparison of film cooling effectiveness with that of previous results for η vs M .

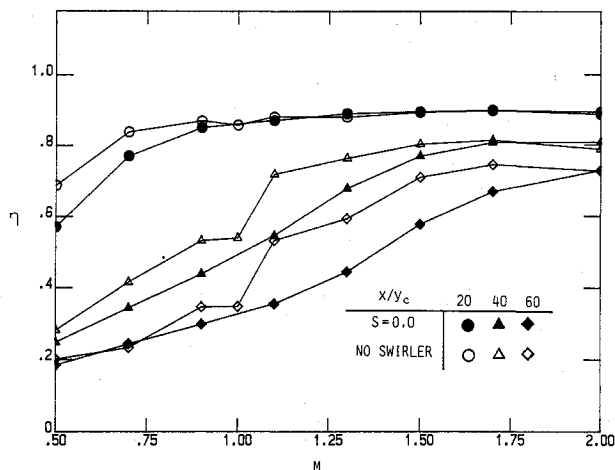


Fig. 6 Comparison of film cooling effectiveness between the case with swirler having $S = 0$ and the case without swirler.

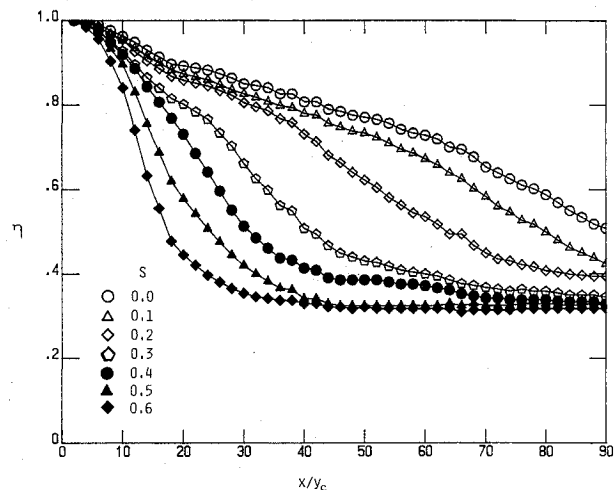


Fig. 7 Effect of swirl on the film cooling effectiveness along the wall at $M = 2.0$.

stant value at a very high blowing parameter. The occurrence of local maximum in film cooling effectiveness in the pipe without expansion does not appear in the pipe downstream of an expansion. The maximum in film cooling effectiveness occurs when the mixing rate between the film jet and the mainstream is the least, i.e., when the blowing parameter is close to unity and the velocity difference between the film jet and the mainstream is almost zero.¹ In the present experiment, a recirculation zone forms between the film jet and the mainstream and the least mixing rate of the film jet with the mainstream is not found. In the present experiment, the maximum uncertainty of the film cooling effectiveness is $\pm 8.3\%$, which is calculated by the method reported by Kline and McClintock.²² It is also found that with the insertion of the thermocouple rake, the film cooling effectiveness remains essentially the same.

Effect of Guide Cone

When the swirler that has a 0-deg vane angle is situated upstream, the mainstream can be significantly disturbed by the swirler. The flow velocity can be accelerated by the guide cone and significantly distorted by the swirl vane and the hub. A wake region can be generated behind the hub. By calculating the area blocked by the swirl hub, the guide cone can accelerate the inlet flow velocity by 20%. After passing through the swirler, the flow decelerates. It is expected that the significant disturbance of inlet flow velocity by the swirler can have a profound influence on the film cooling effectiveness.

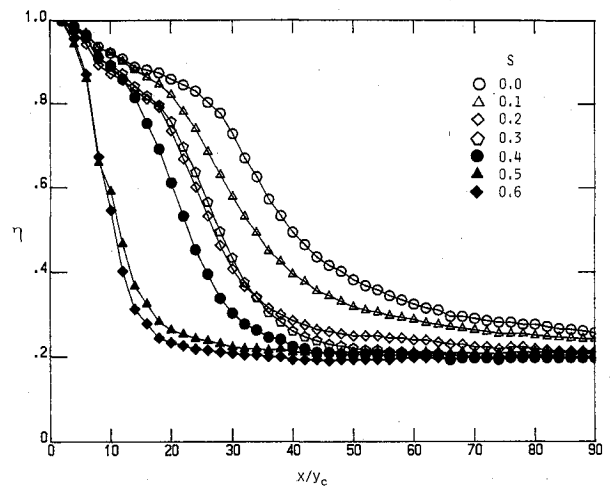


Fig. 8 Effect of swirl on the film cooling effectiveness along the wall at $M = 1.0$.

The film cooling effectiveness for the case of flow where the swirler is absent and the case where a swirler that has a 0-deg vane angle is situated upstream is compared in Fig. 6. It appears that the effect of flow disturbance, due to the presence of a swirler, on the film cooling effectiveness is not significant in the near slot region and becomes significant in the downstream region for moderate blowing parameters ($1.0 \leq M \leq 1.7$). However, for the case of film cooling without pipe expansion, the presence of the same swirler in the mainstream does not have a significant effect on the film cooling effectiveness.⁹ It appears that for the present case the reduction of the film cooling effectiveness is attributed to the disturbed flow, which reduces the size of the recirculation zone, moves the point of reattachment upstream, and causes an earlier destruction of the film jet structure.

At low blowing parameters, the film jet has been destroyed severely in the downstream region, therefore, the reattachment of flow does not have a significant effect on the film cooling effectiveness. At high blowing parameters, the high axial momentum of the film jet can move the reattachment point further downstream and at the same time protect the film jet from the detrimental entrainment of the mainstream. Therefore, a moderate reduction of the film cooling effectiveness is found only in the downstream region and in the moderate blowing parameter range.

Effect of Swirl Number and Blowing Parameter

With the presence of swirl, the film cooling effectiveness decreases inversely in proportion to the swirl number, as shown in Figs. 7 and 8, at different blowing parameters. The experiment confirms the previous analysis that the swirl number can be used as a parameter to correlate the film cooling effectiveness. The reduction in the film cooling effectiveness is attributed to the swirl flow, which can reduce the size of the recirculation zone, can move the reattachment point upstream, and can cause an earlier destruction of the film jet structure. The higher the swirl number, the easier the film jet structure is destroyed and the lower the film cooling effectiveness. A complete destruction of the film jet structure at a high swirl can be concluded when the film cooling effectiveness reaches a constant value. In general, it is found that the higher the swirl, the lower the blowing parameter, and the earlier (lower) the film cooling effectiveness reaches a constant value. The complete destruction of film jet structure is also concluded from the temperature distribution measurements. The constant value of film cooling effectiveness in the downstream region has never been found for the case of uniform flow over a film cooled surface.¹ Similar results for the case of the swirling flow without expansion were obtained. However, the reduction in the film cooling effectiveness is attributed to the

strong turbulence intensity and swirl velocity generated by the swirl vane, which can rapidly increase the mixing rate of the film jet with the mainstream.

Figure 9 indicates that film cooling effectiveness increases significantly at a certain range of blowing parameters and reaches a constant value thereafter. No maximum in the film cooling effectiveness is found due to the formation of the

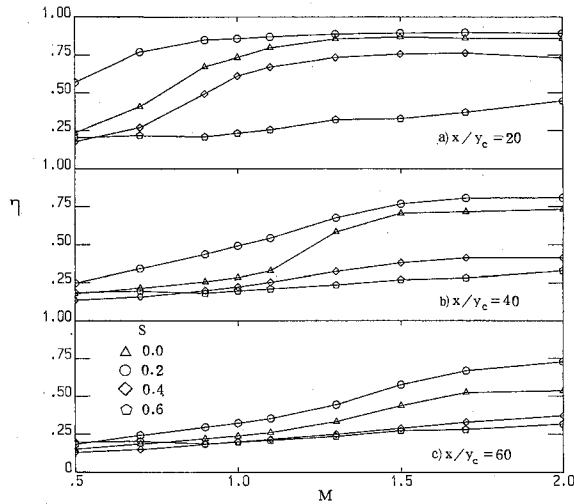


Fig. 9 Effect of swirl on the film cooling effectiveness as a function of blowing parameter: a) $x/y_c = 20$; b) $x/y_c = 40$; and c) $x/y_c = 60$.

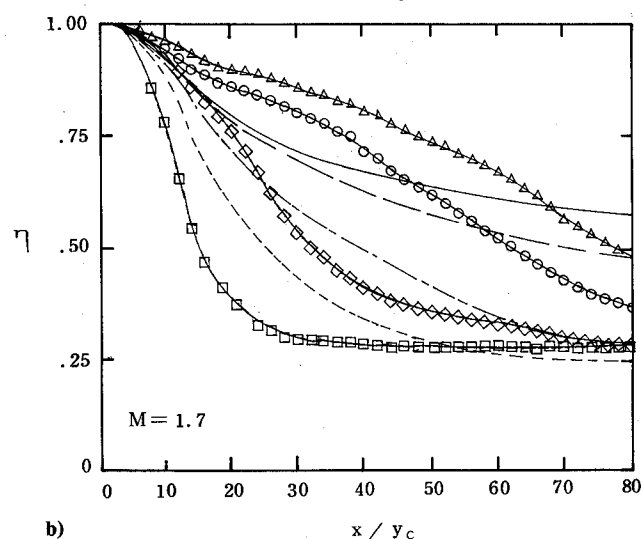
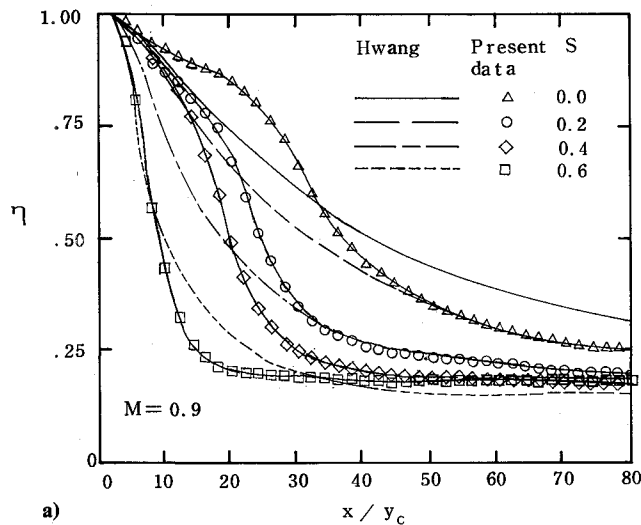


Fig. 10 Effect of sudden expansion: a) $M = 0.9$; b) $M = 1.7$.

recirculation zone, which precludes the occurrence of the least mixing rate of the film jet with the mainstream when the blowing parameter is close to unity.

Effect of Sudden Expansion

The film cooling effectiveness for the case of swirl flow in the mainstream from the present data is shown in Fig. 10 and is compared with that of a film cooled pipe without expansion.⁹ When the swirl number is small, the film cooling effectiveness for the case with expansion is higher in the near slot region and lower in the downstream than the case without expansion. The findings are very similar to the results described previously when the swirl is not present. When the swirl number increases, the swirl makes the recirculation zone shrink, moves the reattachment point upstream, and causes the destruction of film jet structure at an earlier stage. The upstream movement of the reattachment point can also be inferred from the upstream movement of the intersection of the effectiveness curves when the swirl number increases gradually, as shown in Figs. 10a and 10b. It appears that the small recirculation zone becomes intense at high blowing parameter and can enhance the mixing with the film jet. Therefore, it results in a lower film cooling effectiveness than the case without expansion. However, in the downstream region, the film cooling effectiveness for both cases approaches essentially the same constant value. When the blowing parameter increases, the reattachment point moves downstream, which can be inferred from the downstream movement of the inter-

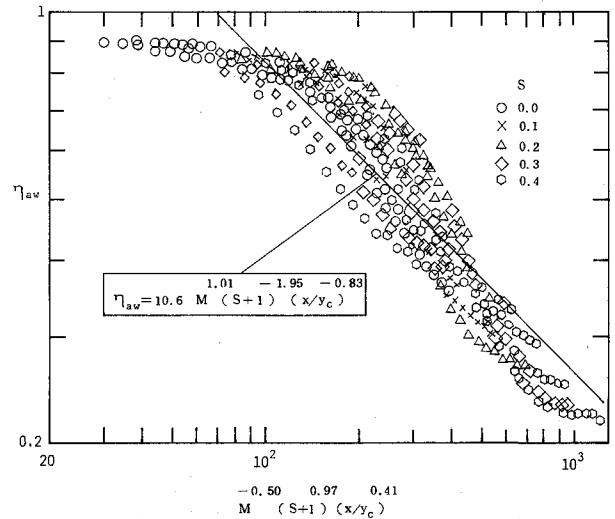


Fig. 11a Film cooling effectiveness correlation for $0.5 \leq M \leq 1.1$, $0.0 \leq S \leq 0.4$, $20 \leq x/y_c \leq 60$.

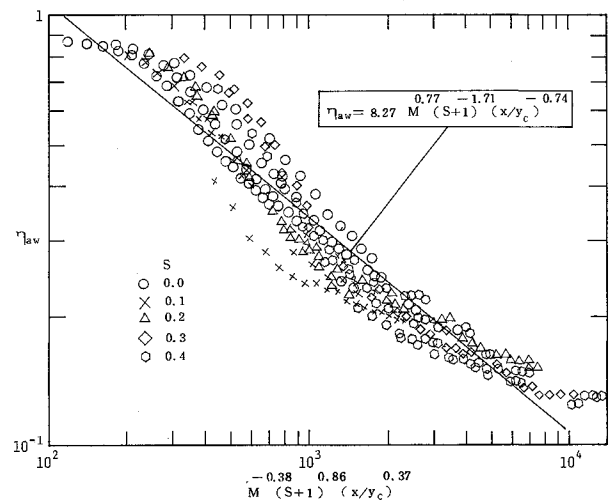


Fig. 11b Film cooling effectiveness correlation for $1.1 < M \leq 2.0$, $0.0 \leq S \leq 0.4$, $20 \leq x/y_c \leq 60$.

section point. However, it has been concluded from the temperature distribution measurements that the size of the recirculation zone decreases when the blowing parameter increases. Therefore, the shrinking of the recirculation zone does not prevent the occurrence of a high film jet velocity from moving the reattachment point downstream. It appears that the recirculation zone becomes thinner and longer when the blowing parameter increases and the swirl is present in the mainstream.

Correlation Results

In the previous nondimensional analysis, the film cooling effectiveness is shown to be a function of the blowing parameter M , the slot Reynolds number Re_s , the downstream distance x/y_c , and the swirl number S . However, the experimental results¹⁵ indicate that the slot Reynolds number in the range from 1960 to 6550 does not affect the film cooling effectiveness significantly. Therefore, the slot Reynolds number is excluded and the film cooling effectiveness data are correlated with the following parameters: the blowing parameter M , the downstream distance x/y_c , and the swirl number S . The film cooling effectiveness data are divided into two correlating regions: the region for low blowing parameter $M \leq 1.1$ and that for high blowing parameter $M > 1.1$. To obtain a better correlation, all of the data for $S \geq 0.5$ are deleted. The results from a least-square fit of data are given as follows:

For $0.5 \leq M \leq 1.1$, $20 \leq x/y_c \leq 60$, $0.0 \leq S \leq 0.4$

$$\eta_{aw} = 10.6M^{1.01}(S+1)^{-1.95}(x/y_c)^{-0.83} \quad (10)$$

with a standard deviation of 0.0538.

For $1.1 < M \leq 2.0$, $20 \leq x/y_c \leq 60$, $0.0 \leq S \leq 0.4$

$$\eta_{aw} = 8.27M^{0.77}(S+1)^{-1.71}(x/y_c)^{-0.74} \quad (11)$$

with a standard deviation of 0.1036.

Comparisons of the correlations with the data are shown in Figs. 11a and 11b, respectively.

Conclusions

Weak swirling flow through a pipe with expansion has a significant effect on the film cooling performance. The recirculation zone and the reattachment of flow that occurred in the upstream region play a significant role in affecting the mixing process of the film jet with the mainstream. The radial temperature measurements are used to infer the flow structure and the rate of mixing of the film jet with the mainstream. The swirl can reduce the recirculation zone and increase the mixing rate of the film jet with the mainstream. The reattachment of flow in the near slot region can significantly destroy the film jet structure and reduce the film cooling effectiveness. In the downstream region, the film cooling effectiveness approaches a constant value. A complete mixing of the film jet with swirl flow can be concluded from the temperature distribution and adiabatic wall temperature measurements. The nondimensional parameters that affect the film cooling performance are derived analytically and confirmed experimentally. Correlations for film cooling effectiveness downstream of an abrupt expansion, taking into account the effect of swirl, are presented.

References

- ¹Lefebvre, A. H., *Gas Turbine Combustion*, Hemisphere, Washington, DC, 1983, pp. 286-299.
- ²Goldstein, R. J., "Film Cooling," *Advances in Heat Transfer*, Vol. 7, edited by J. P. Hartnett and T. F. Irvine Jr., Academic Press, New York, 1971, pp. 321-379.
- ³Seban, R. A., and Back, L. H., "Effectiveness and Heat Transfer for a Turbulent Boundary with Tangential Injection and Variable Free-Stream Velocity," *Journal of Heat Transfer*, Vol. 84, No. 1, 1962, pp. 235-244.
- ⁴Hay, N., Lampard, D., and Saluja, C. L., "Effect of the Condition of the Approach Boundary and of Mainstream Pressure Gradients on the Heat Transfer Coefficient on Film Cooled Surfaces," *Journal of Engineering for Gas Turbines and Power*, Vol. 107, No. 1, 1985, pp. 99-104.
- ⁵Marek, C. J., and Tacina, R. R., "Effects of Free-Stream Turbulence on Film Cooling," NASA TN D-7985, June 1975.
- ⁶Carlson, L. W., and Talmor, E., "Gaseous Film Cooling at Various Degrees of Hot-Gas Acceleration and Turbulence Levels," *International Journal of Heat Mass Transfer*, Vol. 11, No. 11, 1968, pp. 1695-1713.
- ⁷Goldstein, R. J., Eckert, E. R. G., Ching, H. D., and Elovic, E., "Effect of Surface Roughness on Film Cooling Performance," *Journal of Engineering for Gas Turbines and Power*, Vol. 107, No. 1, 1985, pp. 111-116.
- ⁸Mayle, R. E., Kopper, F. C., Blair, M. F., and Bailey, D. A., "Effect of Streamline Curvature on Film Cooling," *Journal of Engineering for Power*, Vol. 99, No. 1, 1977, pp. 77-82.
- ⁹Gau, C., and Hwang, W. B., "Effect of Weak Swirling Flow on Film Cooling Performance," *ASME Journal of Turbomachinery*, Vol. 112, No. 4, 1990, pp. 786-791.
- ¹⁰Beer, J. M., and Chigier, N. A., *Combustion Aerodynamics*, Krieger, Malabar, FL, 1983, pp. 85-146.
- ¹¹Syred, N., and Beer, J. M., "Combustion in a Swirling Flow: A Review," *Combustion and Flame*, Vol. 23, No. 2, 1974, pp. 143-201.
- ¹²Faler, J. H., and Lebovich, S., "Disrupted States of Vortex and Vortex Breakdown," *Physics of Fluids*, Vol. 20, No. 9, 1977, pp. 1385-1400.
- ¹³Dellenback, P. A., Metzger, D. E., and Neitzel, G. P., "Heat Transfer to Turbulent Swirling Flow Through a Sudden Axisymmetric Expansion," *Journal of Heat Transfer*, Vol. 109, No. 3, 1987, pp. 613-620.
- ¹⁴Habib, M. A., and McEligot, D. M., "Turbulent Heat Transfer in a Swirl Flow Downstream of an Abrupt Pipe Expansion," *Proceedings of the 7th International Heat Transfer Conference*, Munich, Germany, Vol. 3, edited by V. Grigull, E. Hahne, K. Stephan, and I. Straub, Hemisphere, Washington, DC, 1982, pp. 159-165.
- ¹⁵Chang, S. S., "Film Cooling in a Can-Type Combustor," M.S. Thesis, National Cheng Kung Univ., Taiwan, 1989.
- ¹⁶Zemanick, P. P., and Dougall, R. S., "Local Heat Transfer Downstream of Abrupt Circular Channel Expansion," *Journal of Heat Transfer*, Vol. 92, No. 1, 1970, pp. 53-60.
- ¹⁷Baughn, J. W., Hoffman, M. A., Takahashi, R. K., and Launder, B. E., "Local Heat Transfer Downstream of an Abrupt Expansion in a Circular Channel with Constant Wall Heat Flux," *Journal of Heat Transfer*, Vol. 106, No. 4, 1984, pp. 789-796.
- ¹⁸Lilley, D. G., "Swirl Flow in Combustion: A Review," *AIAA Journal*, Vol. 15, No. 8, 1977, pp. 1063-1078.
- ¹⁹Gupta, A. K., Lilley, D. G., and Syred, N., *Swirl Flow*, Abacus, Tunbridge Wells, UK, 1984, pp. 119-218.
- ²⁰Bach, T. V., and Gouldin, F. C., "Flow Measurements in a Model Swirl Combustor," *AIAA Journal*, Vol. 20, No. 5, 1982, pp. 642-651.
- ²¹Ko, S. Y., and Liu, D. Y., "Experimental Investigation on Effectiveness, Heat Transfer Coefficient, and Turbulence of Film Cooling," *AIAA Journal*, Vol. 18, No. 8, 1980, pp. 907-912.
- ²²Kline, S. J., and McClintock, F. A., "Describing Uncertainties in Single-Sample Experiments," *Mechanical Engineering*, Vol. 73, No. 1, 1953, pp. 3-8.